DOI: XXX-XXX-XXXX

Modeling and Fault Tolerant Control of an Electro-Hydraulic Actuator

Syed Abu Nahian[1], Dinh Quang Truong[1] Puja Chowdhury[1] Debdatta Das[1], and Kyoung Kwan Ahn [2,#]

1 Graduated School of Mechanical Engineering, University of Ulsan, Daehakro 93, Namgu, Ulsan, South Korea,680-749
2 School of Mechanical Engineering, University of Ulsan, Daehakro 93, Namgu, Ulsan, South Korea,680-749
Corresponding Author / E-mail: kkahn@ulsan.ac.kr, TEL: +82-52-259-2282 , FAX: +82-52-259-1680

KEYWORDS : Electro-hydraulic actuator, Sensor fault, Fault tolerant control, Unknown input observer, BELBIC

In the modern industry, electro-hydraulic actuators (EHAs) have been applied to various applications for precise position pressure/force control tasks. However, operating EHAs under sensor faults is one of the critical challenges for the control engineers. For its enormous nonlinear characteristics, sensor fault could lead the catastrophic failure to the overall system or even put human life in danger. Thus in this paper, a study on mathematical modeling and fault tolerant control (FTC) of a typical EHA for tracking control under sensor-fault conditions has been carried out. In the proposed FTC system, the extended Kalman-Bucy unknown input observer (EKBUIO) -based robust sensor fault detection and identification (FDI) module estimates the system states and the time domain fault information. Once a fault is detected, the controller feedback is switched from the faulty sensor to the estimated output from the EKBUIO owing to mask the sensor fault swiftly and retains the system stability. Additionally, considering the tracking accuracy of the EHA system, an efficient brain emotional learning based intelligent controller (BELBIC) is suggested as the main control unit. Effectiveness of the proposed FTC architecture has been investigated by experimenting on a test bed using an EHA in sensor failure conditions.

Manuscript received: August XX, 201X / Revised: August XX, 201X / Accepted: August XX, 201X

NOMENCLATURE

A_h = head side piston area
A_r = rod side piston area
A_v = valve opening area
C_v = valve discharge coefficient
D = pump displacement
d_k^s = position sensor fault information of EHA
E_{max} = the bulk modulus of the hydraulic fluid
frc = friction force between cylinder wall and piston
F_{load} = applied load on the cylinder
l = cylinder length
m = piston mass
N = pump rotation per minute (RPM)
P_1 = pump pressure
P_h = head side pressure
P_r = rod side pressure
P_{rel} = relief valve settling pressure
ρ = hydraulic fluid density
Q_{pump} = pump flow rate
V_c = control voltage of the servo motor
x_p = cylinder piston position
Q_1 = inlet flow rate to the cylinder
Q_2= outlet flow rate from the cylinder
Q_{rel} = flow rate through relief valve

1. Introduction

Electro hydraulic actuators are one of the widely accepted solutions in modern industries. With a wide range of applications like heavy duty excavation or the precise operations like computerized numerical control, it has been considered as a potential choice owing to its compact size, high power to weight ratio and small power consumption. For an example, highly efficient EHAs from Moog, Inc. (East Aurora, New York) were validated in real time simulators in terms of accuracy and fast response [1]. In addition, Rahmfeld and Ivantysynova [2] derive the effectiveness of EHAs mathematically. Such especial features increase the popularity of EHAs over the electric motor driven

actuators in current era. Despite the benefits of the EHAs, these are one of the critical nonlinear systems. It is a challenge for control engineers to control nonlinear systems under varieties of working environments and loads. The system performances are then depended on the adaptability of the controller, and especially the reliability of the sensors.

In a closed-loop control system, faults could be raised either in sensors or actuators. For instance, in sophisticated plants like power plants, chemical process plants, fatal accident may occur due to system fault [3, 4]. Subsequently, with the development of smart machines and systems, safe operations and diagnosis of the malfunctions with desirable performances are becoming important aspects with time. Therefore, researchers have been showing interests to develop fault diagnosis algorithm (FDA) in various applications in recent years [5-9]. In parallel, by adopting control laws with the FDA, one can realize the FTC for any system.

In general, the FTC is a control methodology that ensures the safe operation under acceptable limit of a system when faults occur under FDI system. The FDI problem consists of two sub modules: binary decision making (fault detection) and finding the time variant fault behavior (fault identification). Several procedures were conducted by different researchers for fault detection mechanisms. Chi and Zhang [10] proposed a fault detection method based on failure and non-failure hypothesis of an aircraft system. Parameter estimation is also a way for fault detection [11]. This is done by measuring the input and output signals if the basic model structure is known. Then the process follows direct estimation or numerical optimization. In another case, passive robust fault detection was presented by Puig and Quevedo [12] by bounding the uncertainties in intervals, known as 'interval model'. Process model-based fault detection was also evaluated using residual analysis [13]. Meanwhile, observer-based fault identification was carried out by different researchers [14, 15]. These conducted researches reflect the effectiveness of the FDI in fault tolerant control systems.

In today's industry, sensor fault is one of the most important issues that could be occurred at any time without screening any previous symptoms. Especially, a process operated by a nonlinear EHA has potential probability of occurring sensor faults due to high operating pressures or tough working environments or even external impacts on the sensors. For example, sensor faults could be happened in accelerometers of aircraft [16], position sensors [13], sensors in heavy duty tele-operated demolition or excavation robots or hydraulic press load cells due to fatigues, fluctuations of hydraulic fluid, external impacts on sensors or human errors. Such failures lead the controllers to produce wrong control signals which may degrade significantly the overall performances or even put the human life in endanger. Therefore, sensor FTC is becoming one of the firing issues in modern control of EHAs.

In sensor FTC architecture, evaluation of redundant sensor systems is generally used in most of the applications. For an example, Chan and Hong [17] successfully showed how to classify faults under noise using redundant sensors and a modified kohonen network. Furthermore, linear sensor redundancy analysis-based FTC has been recently carried out by Santhosh [18]. In commercial EHAs like VariStroke-I from Woodward (USA), redundant linear displacement transducers have been used for FTC operation. However, the sensor redundancy increases the hardware and FDI designing complexity as well as cost, weights, maintenance effort. Therefore, researchers focused the spot light on the analytical redundancy over hardware redundancy for designing FTC architectures. For an instance, analytical redundancy-based fault diagnosis method by developing a filter with sequential probability ratio test was proposed by Chi and Zhang [10]. In an EHA positioning system, such FTC was carried out by Navid and Nariman [19]. They developed quantitative feedback-based FTC module in which the system was identified by single-input-single-output transfer function. However, the identification of such nonlinear systems with this manner is not feasible. Also, they could not reveal the fault information invoked at the sensors.

Intelligent approaches, like fuzzy, genetic algorithm (GA) and neural network, have been found for FTC in EHA applications. FTC of an electro hydraulic servo axis was studied by Beck and Mark [13] with fuzzy logic-based fault diagnosis. Mendonca and Sousa [20] presented a multiple fuzzy fault model-based FTC and verified it through simulations of a three-tank hydraulic system. Although the simulated fault diagnosis performance was feasible, the excessive fuzzy-based fault model with high degree of expert knowledge as well as large number of parameters increased the computational complexity. Later on, Shang [21] proposed an intelligent fault classification method based on GA and back propagation technique applied to a transmission system. This employed an improved genetic search with fast Fourier transformation (FFT) to solve high dimensional feature selection problem with low computational complexity. Nevertheless, the system vibration and speed signals were required for spectral transformation that involved lots of experimental tests.

Another technique based on system models and observers have been widely used in various applications [6, 7, 14, 22-24]. In EHA applications, several researches [13, 25, 26] have been conducted with observer-based fault diagnosis. Among them, unknown input observer (UIO)-based fault detection is one of the famous methods in FTC. Previous studies [7, 15, 27] showed how this observer

DOI: XXX-XXX-XXXX

detects, isolates and identifies the sensor faults effectively. However in most cases, these researches were conducted without practical verification and sensor/process noises were omitted while large categories of the real systems are stochastic. The extended Kalman filter (EKF) can be a good solution to deal with the stochastic system. Haldar [28] showed a procedure to detect and isolate the sensor fault of an EHA system using conventional EKF. However, the time domain fault information could not be revealed with this approach.

From the above analysis, this paper develops an effective sensor fault tolerant control for an EHA-driven cylinder. The main objective is to control precisely the cylinder position while additive or multiplicative fault is invoked in the system sensors during operation. The FTC architecture is designed with two modules: FDI module and main control module. An unknown input observer adopting with extended Kalman-Bucy filter, called EKBUIO, is proposed as the FDI module. This module takes part in estimating the system states and the unknown input: sensor fault. Using the estimated time domain fault information, threshold-based decisions are then made for fault detection in the EHA system. In order to control the system effectively, an adaptive and computationally efficient online brain emotional learning-based intelligent controller (BELBIC) has been suggested as the main control module. The architecture is realized on the model to mimic those parts of the brain which are known to produce emotion [29]. Consequently being different from the conventional closed-loop architecture having only single control module, the proposed FTC approach possesses both the adaptive control solution and robust fault tolerant methodology to meet the requirement of an effective EHA control performance under sensor faults. An EHA apparatus is setup and, the experimental investigation has been carried out in order to validate the effectiveness of the FTC system in faulty conditions.

This paper is sketched as follows: in Section 2, the overall description of the EHA apparatus has been introduced at first. Then the mathematical modeling of the test bed and the system parameter estimation are studied in Section 3. In Section 4, the developed FTC controller with trajectory control strategy is discussed comprehensively. The experimental investigations are carried out in Section 5 to evaluate the effectiveness of the proposed FTC system applied into EHA. Finally, the conclusion is drawn in Section 6.

2. EHA Apparatus

In this section, the outline of the overall EHA setup is presented.

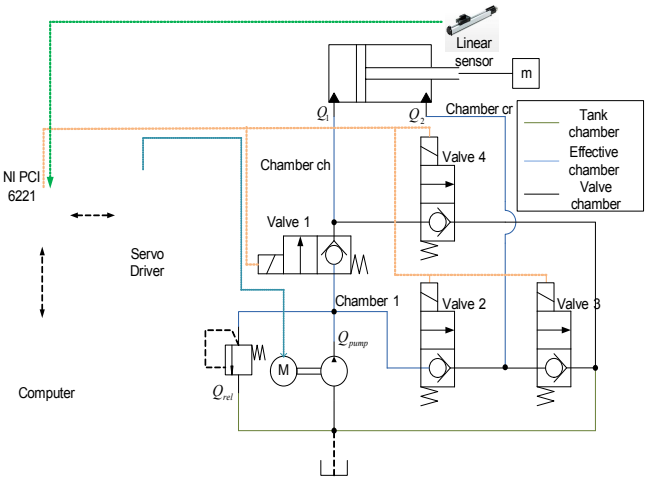

Fig. 1 Configuration of the EHA test rig

Fig. 1 shows the system configuration. As seen in Fig. 1, the EHA system includes hydraulic cylinder driven by a three-phase servo motor and a hydraulic pump with one direction and fixed displacement through a hydraulic valve circuit. This valve circuit consists of four high-speed ON/OFF solenoid controlled valves and one safety pressure regulating valve to perform all operations of the cylinder. The advantages of using a four-valve configuration, such as velocity control or energy saving, has been clearly presented by Shenouda [30]. By this concept, the pressurized flow from the pump can be transmitted to the cylinder to follow the desired tasks by smoothly selecting five modes [30].

In this study, only cylinder power extraction (PE) and power retraction (PR) modes are considered for developing the FTC approach. A personal computer (PC) with compatible specifications

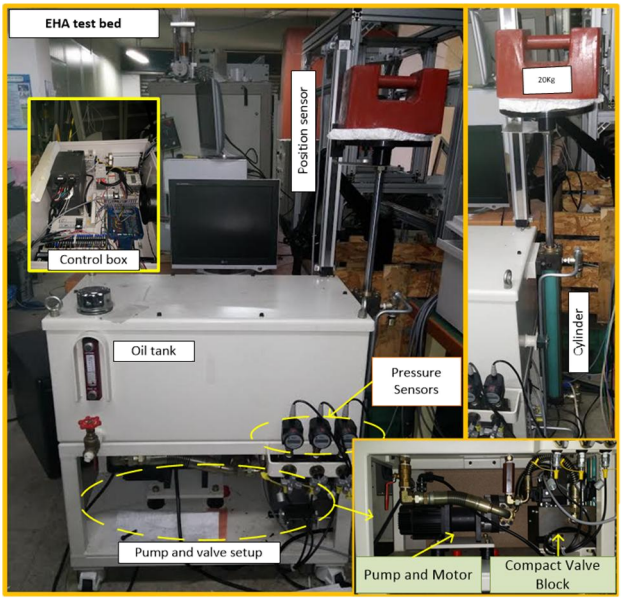

Fig. 2 Experimental EHA test bed

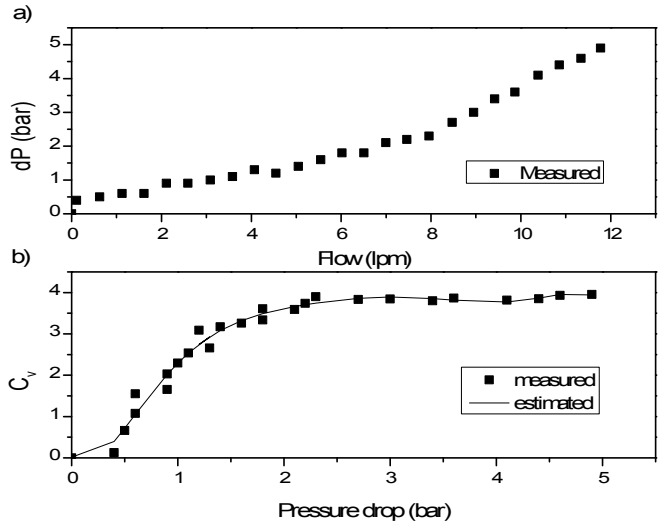

Fig. 3 a) *dP-Q* curve b) *Cv-dP* curve

3. System modeling and identification

3.1 System modeling

The mathematical modeling of the EHA described in the previous section is elaborated in this part. As the valves and servo motor are fast in response, the dynamics are assumed to be linear for the sake of simplicity. The pump flow rate can be calculated as

$$\begin{aligned} Q_{pump} &= DN \\ N &= k_s V_c \end{aligned} \tag{1}$$

where: k_s is a proportional parameter, which defines the RPM to voltage ratio of the servo motor. Now, the momentum equation is

$$m\ddot{x}_p = (A_h P_h - A_r P_r) - F_{load} - frc \tag{2}$$

Theoretically, the bulk modulus E_{max} is the ratio of the change in pressure to the fractional change in volume of any chamber and can be assumed as its mean value given common pressures and temperatures. However in practice, this can be substantially lowered by entrained gas and mechanical compliance. In this study (Fig. 1), it can be represented as a sensitive pressure-domain function [31]. By considering the entrained air and mechanical compliance, the empirical effective bulk moduli of the divided chambers, β_{c1}, β_{ch} and β_{cr} are computed as

$$\begin{aligned} \beta_{c1} &= E_{\max}(1 - e^{(0.4-2\times10^7 P_1)}) \\ \beta_{ch} &= E_{\max}(1 - e^{(0.4-2\times10^7 P_h)}) \\ \beta_{cr} &= E_{\max}(1 - e^{(0.4-2\times10^7 P_r)}) \end{aligned} \tag{3}$$

The flows and continuity equations through the circuit can be expressed as (4) and (5) respectively [32].

$$\begin{aligned} Q_{rel} &= \begin{cases} c_{vr} A_v \sqrt{\dfrac{2|P_1|}{\rho}} sign(P_1) & if\ P_1 > P_{rel} \\ 0 & otherwise \end{cases} \\ Q_1 &= a_1 c_{v1} A_v \sqrt{\frac{2|P_1 - P_h|}{\rho}} sign(P_1 - P_h) \\ &\quad - a_2 c_{v2} A_v \sqrt{\frac{2|P_h|}{\rho}} sign(P_h) \\ Q_2 &= a_3 c_{v3} A_v \sqrt{\frac{2|P_r|}{\rho}} sign(P_r) \\ &\quad - a_4 c_{v4} A_v \sqrt{\frac{2|P_1 - P_r|}{\rho}} sign(P_1 - P_r) \end{aligned} \tag{4}$$

$$\begin{aligned} \frac{dP_1}{dt} &= \frac{\beta_{c1}}{V_{c1}}(a_1(Q_{pump} - Q_1 - Q_{rel}) \\ &\quad + a_2(Q_{pump} + Q_2 - Q_{rel})) \\ \frac{dP_h}{dt} &= \frac{\beta_{ch}}{V_{ch} + x_p A_h}\left(Q_1 - \dot{x}_p A_h\right) \\ \frac{dP_r}{dt} &= \frac{\beta_{ch}}{V_{cr} + (l - x_p) A_r}\left(\dot{x}_p A_r - Q_2\right) \end{aligned} \tag{5}$$

where: V_{c1}, V_{ch}, V_{cr} are the internal constant pipe volumes of 'Chamber 1', 'Chamber ch' and 'Chamber cr' respectively and

$$\left.\begin{aligned} a_1 = 1; a_3 = 1 \\ a_2 = 0; a_4 = 0 \end{aligned}\right\} \quad \forall \dot{x}_p > 0$$

$$\left.\begin{aligned} a_1 = 0; a_3 = 0 \\ a_2 = 1; a_4 = 1 \end{aligned}\right\} \quad \forall \dot{x}_p \le 0$$

Assuming that the valve discharge coefficients $c_{v1}=c_{v2}=c_{v3}=c_{v4}=C_v$ are the same, due to the same valve configuration. Certainly, this coefficient C_v is dependent on the flow dynamics of the valve including flow conditions, laminar or turbulent, deferential pressure, *dP*, valve opening area, A_v and fluid density ρ. For the sake of simplicity, the fluid density can be taken as a constant and because of using high-speed ON/OFF solenoid controlled valves in the EHA, the effect of changing valve area is considered very low and can be neglected as well. Thus the C_v is defined by investigating the relationship between the pressure drop, *dP*, and flow rate, *Q*, of each valve as presented in Fig. 3(a). The tendency of C_v over *dP* is then illustrated as Fig. 3(b) and, finally, approximated by a polynomial function using interpolation technique [33] as follows

$$\begin{aligned} C_v = &-1.100\times10^{-2} dP^7 + 2.040\times10^{-1} dP^6 - 1.5263\, dP^5 + 5.8795\, dP^4 \\ &- 12.17865832\, dP^3 + 12.146\, dP^2 - 2.204\, dP - 1.890\times10^{-2} \end{aligned} \tag{6}$$

The friction load presented in (2) can be modeled as [31],

$$frc = \begin{cases} \sigma_u \dot{x}_p + Sign(\dot{x}_p)(F_{cu} + F_{su} e^{\left(\frac{-|\dot{x}_p|}{C_{su}}\right)}) & \forall \dot{x}_p > 0 \\ \sigma_d \dot{x}_p + Sign(\dot{x}_p)(F_{cd} + F_{sd} e^{\left(\frac{-|\dot{x}_p|}{C_{sd}}\right)}) & \forall \dot{x}_p < 0 \end{cases} \tag{7}$$

DOI: XXX-XXX-XXXX

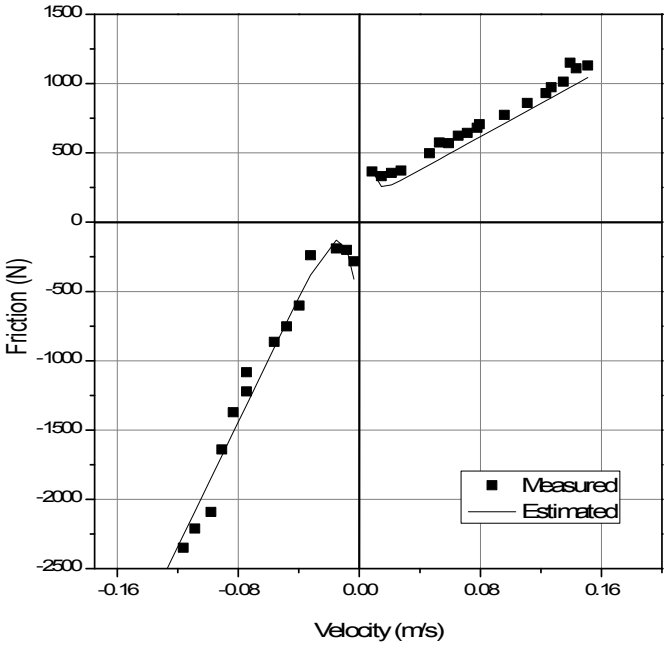

Fig. 4 Friction force vs. cylinder speed.

here: σ_u and σ_d are the viscous friction parameters; F_{cu} and F_{cd} are the coulomb frictions; F_{su} and F_{sd} are the static friction forces ; C_{su} and C_{sd} are known as Stribeck velocity parameters for the 'up' and 'down' motion of the cylinder, respectively. Subsequently, based on the dynamic equations from (1) to (7), the system can be represented by a state vector $[x_1 \;\; x_2 \;\; x_3 \;\; x_4 \;\; x_5]^T = [\dot{x}_p \;\; x_p \;\; P_1 \;\; P_h \;\; P_r]^T$ and can be expressed as

$$\begin{bmatrix} \dot{x}_1 \\ \dot{x}_2 \\ \dot{x}_3 \\ \dot{x}_4 \\ \dot{x}_5 \end{bmatrix} = \begin{bmatrix} \frac{1}{m}(A_1 x_4 - A_2 x_5 - frc) \\ x_1 \\ -\frac{\beta_{c1}}{V_1}(a_1 Q_1 - a_2 Q_2) \\ \frac{\beta_{ch}}{V_h + x_2 A_1 1000}(Q_1 - x_2 A_1 \cdot 1000) \\ \frac{\beta_{cr}}{V_r + (l - x_2) * A_1 * 1000}(A_2 x_1 \cdot 1000 - Q_2) \end{bmatrix} + \begin{bmatrix} 0 \\ 0 \\ \frac{\beta_{c1}}{V_1} \\ 0 \\ 0 \end{bmatrix} Q_{pump} \quad (8)$$

From (8), it can be seen that the presented EHA is the complex system with nonlinear dynamic terms. Moreover, as the developed FTC scheme (see Section 4) relies on the extended Kalman-Bucy filter, the state estimation performance can get advantages from the system description with minimal modeling error. Thus, it is necessary to derive the accurate model. The system parameters can be found either from the manufacture provided datasheet or can be identified experimentally. In this paper, the observed and known terms are listed in Table 1. On the other hand, some unobserved terms like the chamber volumes, friction coefficients, valve parameters and RPM to voltage ratio parameter can be derived by performing a parameter optimization procedure which is discussed in the next subsection.

Table 1 EHA physical parameters

Components	values	Unit
A_h	0.00126	m^2
A_r	0.00088	m^2
A_v	2.54×10^{-6}	mm^2
D	16.3	cm^3
F_{load}	20	Kgf
m	0.43	Kg
E_{max}	1.5×10^{9}	Pa
ρ	870	Kg/m^3
P_{rel}	40	bar
l	500	mm

Table 2 Optimized model parameters

Parameters	Identified values	Unit
V_{c1}	0.1996	L
V_{ch}	0.0394	L
V_{cr}	0.201	L
σ_u	5915.8	Ns/m
σ_d	22554	Ns/m
F_{cu}	28.62	N
F_{cd}	364.02	N
F_{su}	774.12	N
C_{su}	0.00012	m/s
C_{sd}	0.007541	m/s
k_s	300	RPM/V

3.2 Parameter estimation

Here, the unobserved parameters were estimated by offline tuning method with Matlab/Simulink parameter estimation toolbox. First based on the friction-velocity relationship (Fig. 4) derived from the experiments, the friction parameters σ_u , σ_d , F_{cu}, F_{cd}, F_{su}, F_{sd}, C_{su} and C_{sd} were identified. Next, with the identified friction model, the constant volumes, V_{c1}, V_{ch}, V_{cr} and the proportional parameter k_s were estimated based on a random set of input/output data of the EHA. Fig. 5 displays the comparison between the model output and actual response of the cylinder corresponding to arbitrary input signals of the motor and valves. This result shows that the model with optimized parameters could represent well the actual system

with adequate accuracy. Finally, the estimated system parameters are summarized in Table 2.

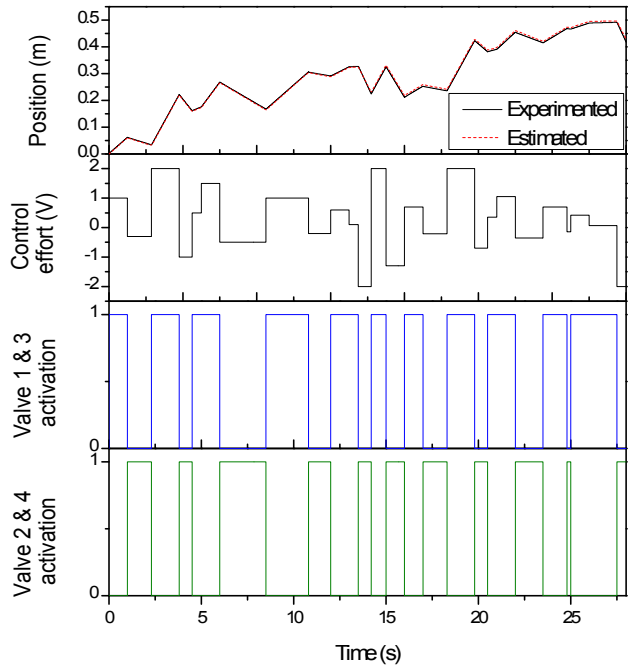

Fig. 5. Comparison between model output and actual system response.

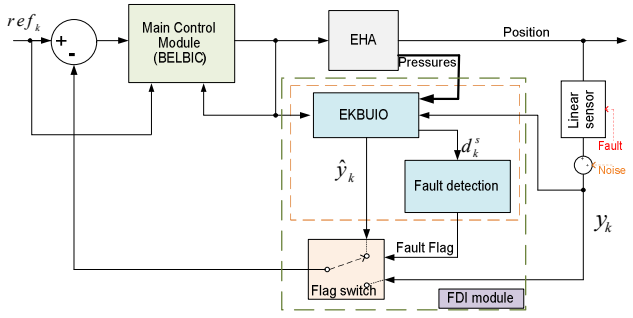

Fig. 6 Position control configuration of EHA with sensor FTC

4 FTC design for EHA

The proposed FTC system for EHA system has been demonstrated in Fig. 6. In operation, the BELBIC acts as the main controller and performs conventional closed-loop trajectory control. Once the fault detection is made (See Section 4.2) the decision is to switch the feedback from between the sensor and the estimated position output of the EKBUIO using an operator defined as a 'flag switch'. Hence, the sensor fault can be masked and the controller reconfiguration is not required which is a complicated procedure to retain system stability. The design procedures of each module of the FTC system are discussed in next subsections.

4.1 Extended Kalman-Bucy Unknown Input Observer

For a generic system, the unknown input is an undefined time variant characteristic with unbounded amplitude that can be experienced by either sensor or actuator which leads the system instability. Therefore in this paper fault is considered as an unknown input and in this section, the design procedure of unknown input observer based on the extended Kalman-Bucy filter (EKBF) is explained elaborately.

At first, a simple unknown input observer is derived for a linear time invariant system with a form of

$$\dot{x} = Ax + Bu$$
$$y = Cx \tag{9}$$

where: $x \in R^n, y \in R^m, u \in R^r$ are system state vector, output vector, input vector. A, B, C are the known matrices with proper dimensions corresponding to linear, time invariant system state space description. Now in discrete form, the linear system with actuator unknown input and additive noises could be derived as [15]

$$x_{k+1} = A_k x_k + B_k u_k + E_k d_k + w_k \tag{10}$$

$$y_k = C_k x_k + v_k \tag{11}$$

where: $x_k \in R^n, y_k \in R^m, u_k \in R^r, d_k \in R^q$ are discrete time system state vector, output vector, known input vector, unknown input vector representing as fault respectively. w_k, v_k are the zero mean white noise and $A_k = e^{A\tau}, B_k = \tau B \; and \; C_k = C$ are calculated for discretization purpose with τ sampling time.

Considering the unknown input observer in form of

$$z_{k+1} = F_{k+1} z_k + T_{k+1} B_k u_k + K_{k+1} y_k \tag{12}$$

$$\hat{x}_{k+1} = z_{k+1} + H_{k+1} y_{k+1} \tag{13}$$

where: $\hat{x}_{k+1} \in R^n, z_{k+1} \in R^n$ are the estimated state vector and states of the observer. The observer matrixes $F_{k+1}, T_{k+1}, H_{k+1}$ and K_{k+1} should be designed in a way that the state estimation error $e_{k+1} = x_{k+1} - \hat{x}_{k+1}$ asymptotically converses to zero. From (10) to (13), the error term can be derived as

$$\begin{aligned} e_{k+1} = & -[F_{k+1} - (I - H_{k+1} C_{k+1}) A_k + K_{k+1}^1 C_{k+1}] x_k + F_{k+1} e_k \\ & - [K_{k+1}^2 - F_{k+1} H_{k+1}] y_k - [T_{k+1} - (I - H_{k+1} C_{k+1})] B_k u_k \\ & + (I - H_{k+1} C_{k+1}) E_k d_k - H_{k+1} v_{k+1} + (I - H_{k+1} C_{k+1}) w_k - K_{k+1}^1 v_k \end{aligned} \tag{14}$$

where: $K_{k+1} = K_{k+1}^1 + K_{k+1}^2$. Therefore to form the UIO, the following relations must hold.

$$E_k = H_{k+1} C_{k+1} E_k \tag{15}$$

$$\begin{aligned} T_{k+1} &= I - H_{k+1} C_{k+1} \\ F_{k+1} &= T_{k+1} A_k - K_{k+1}^1 C_{k+1} \\ K_{k+1}^2 &= F_{k+1} H_{k+1} \end{aligned} \tag{16}$$

The necessary and sufficient conditions for the observer of the given system are [34]:

1) $rank(C_{k+1} E_k) = rank(E_k)$

2) $(C_{k+1}, T_{k+1} A_k)$ is a detectable pair.

DOI: XXX-XXX-XXXX

Subsequently, one special solution of (15) could be obtained as

$$\begin{aligned} H_{k+1} &= E_{k+1}H_{k+1}^1 \\ H_{k+1}^1 &= (C_{k+1}E_{k+1})^+ \\ &= [(C_{k+1}E_{k+1})^T C_{k+1}E_{k+1}]^{-1}(C_{k+1}E_{k+1})^T \end{aligned} \tag{17}$$

Thus, the state estimation error becomes:

$$e_{k+1} = F_{k+1}e_k - K_{k+1}^1 v_k - H_{k+1}v_{k+1} + T_{k+1}w_k \tag{18}$$

It is obvious that without additional noises and disturbances, e_{k+1} will converse to zero asymptotically if F_{k+1} is stable. So, in order to design the observer, one has to select the stable F_{k+1} by a proper choice of K_{k+1}^1. Another study [35] shows that to derived e_{k+1} with minimum variance the gain matrix can be written as

$$K_{k+1}^1 = T_{k+1}A_k P_k C_k^T [C_k P_k C_k^T + R_k]^{-1} \tag{19}$$

where: the covariance matrices are given by

$$\begin{aligned} P_{k+1} &= T_{k+1}A_k P_{k+1/k} A_{1,k+1}^T + T_{k+1}Q_k T_{k+1}^T + H_{k+1}R_{k+1}H_{k+1}^T \\ P_{k+1/k} &= P_k - K_{k+1}^1 C_k P_k T_{k+1} A_k \end{aligned} \tag{20}$$

Now, the observer can be converted into Kalman filter form in order to estimate the states in the stochastic environment. Now, multiplying (11) with H_{k+1}^1 and inserting in (10) leads

$$d_k = H_{k+1}^1 [y_{k+1} - C_{k+1}(A_k \hat{x}_k + B_k u_k)] \tag{21}$$

From (10) and (21), one has

$$x_{k+1} = \bar{A}x_k + \bar{B}u_k + \bar{E}_k y_{k+1} \tag{22}$$

where:

$$\bar{A}_k = \bar{G}_k A_k \,,\ \bar{B}_k = \bar{G}_k B$$

$$\bar{G}_k = I - E_k H_{k+1}^1 C_{k+1},\ \bar{E}_k = E_k H_{k+1}^1$$

Consequently the unknown input observer for the linear system can be given as [36]

$$\hat{x}_{k+1} = \hat{x}_{k+1/k} + K_{k+1}^1 (y_k - C_k \hat{x}_k) \tag{23}$$

where:

$$x_{k+1/k} = \bar{A}x_k + \bar{B}u_k + \bar{E}_k y_{k+1} \tag{24}$$

Secondly for a nonlinear discrete time invariant system, Witczac and Pretki [37] developed an extended unknown input observer based on EKF algorithm. Let the system is defined as

$$x_{k+1} = g(x_k) + h(u_k) + E_k d_k + W_k \tag{25}$$

$$y_{k+1} = C_{k+1}x_{k+1} + V_k \tag{26}$$

where: $W_k \sim \mathrm{N}(0, Q_k), V_k \sim \mathrm{N}(0, R_k), k \in \mathbb{Z}$ are independent and $g(.), h(.)$ are nonlinear functions. The extended UIO can be expressed as

$$\hat{x}_{k+1} = \hat{x}_{k+1/k} + K_{k+1}^1 (y_{k+1} - C_k \hat{x}_{k+1/k}) \tag{27}$$

Similarly, by multiplying H_{k+1}^1 with (26) and solving with (25) leads the unknown input as

$$d_k = H_{k+1}^1 [y_{k+1} - C_{k+1}(g(x_k) + h(u_k))] \tag{28}$$

By substituting with (25), the prior state can be estimated as

$$\hat{x}_{k+1/k} = \bar{g}(\hat{x}_k) + \bar{h}(u_k) + \bar{E}_k y_{k+1} \tag{29}$$

where:

$$\bar{g}(.) = \bar{G}_k g(.),\ \bar{h}(.) = \bar{G}_k h(.)$$

$$\bar{G}_k = I - E_k H_{k+1}^1 C_{k+1},\ \bar{E}_k = E_k H_{k+1}^1$$

The error covariance matrixes and the Kalman gain can be calculated as

$$P_{k+1/k} = \bar{A}_k P_k \bar{A}_k^T + Q_k \tag{30}$$

$$K_{k+1}^1 = P_{k+1/k} C_{k+1}^T (C_{k+1} P_{k+1/k} C_{k+1}^T + R_{k+1})^{-1} \tag{31}$$

$$P_{k+1} = [I - K_{k+1}^1 C_{k+1}] P_{k+1/k} \tag{32}$$

where: $\bar{A}_k = \dfrac{\partial \bar{g}(x_k)}{\partial x_k} = \bar{G}_k \dfrac{\partial g(x_k)}{\partial x_k}_{|x_k = \hat{x}_k} = \bar{G}_k A_k$

In the above mathematical derivation, the unknown input dk can be considered as an actuator unknown input. Consequently, in order to find the sensor unknown input: the fault in the EHA system position sensor, a subsequent procedure is followed. The nonlinear EHA system is modeled as

$$\begin{aligned} \dot{x}(t) &= f(x(t)) + b(u(t)) + W(t) \\ y_k &= Cx_k + V_k \end{aligned} \tag{33}$$

where: *f(.)* and *b(.)* are the nonlinear functions corresponding to (8) and the observation with the unknown sensor fault with fault distribution matrix E_m can be modeled as

$$\begin{aligned} y_k &= Cx_k + E_m d_k^s + V_k \\ \dot{d}^s(t) &= d^s(t) + \psi(t) \end{aligned} \tag{34}$$

Here, $\psi(t) \in \Re$ is the auxiliary unknown input. Now to design the proposed EKBUIO of the EHA system, consider the augmented system state space representation becomes into

$$\begin{aligned} \underbrace{\begin{bmatrix} \dot{x}(t) \\ \dot{d}^s(t) \end{bmatrix}}_{\dot{X}(t)} &= \underbrace{\begin{bmatrix} f(x(t)) \\ d^s(t) \end{bmatrix}}_{g(X(t))} + \underbrace{\begin{bmatrix} b(u(t)) \\ 0 \end{bmatrix}}_{h(u(t))} + \underbrace{\begin{bmatrix} 0 \\ 1 \end{bmatrix}}_{E_t} \psi(t) \\ y_k &= \underbrace{[C \quad E_m]}_{C_k} X_k \end{aligned} \tag{35}$$

Then, using the form of (29) to (32), the predict and time update equations of the EKBUIO can be formulated as follows

$$\begin{aligned} \dot{\hat{X}}(t) &= \bar{g}(\hat{X}(t)) + \bar{h}(u(t)) + \bar{E}_t y(t) \\ \dot{P}(t) &= \bar{A}_c P(t) + P(t)\bar{A}_c^T + Q_c^a \end{aligned} \tag{36}$$

where:

$$\hat{X}(t_{k-1}) = \hat{X}_{k-1|k-1}$$
$$P(t_{k-1}) = P_{k-1|k-1}$$
$$y(t_{k-1}) = y_{k-1|k-1}$$

$$\bar{A}_c = \frac{\partial \bar{g}(\hat{X}(t))}{\partial X(t)} = \bar{G}_k \frac{\partial g(\hat{X}(t))}{\partial \hat{X}(t)}\bigg|_{\hat{X}(t)}$$
$$\bar{E}_t = E_t H_t$$
$$H_t = [(C_k E_t)^T C_k E_t]^{-1}(C_k E_t)^T$$

Here $\hat{X}_k$ and P_k is the estimated states and the corresponding error covariance matrix of the system presented on (35) at time k. The Kalman gain and covariance matrices are derived by

$$K_k = P_{k|k-1}C_k^T(C_k P_{k|k-1} C_k^T + R_k)^{-1},\ \forall P_{k|k-1} = P(t_k)$$
$$P_k = (I - K_k C_k)P_{k|k-1} \quad (37)$$

Finally, the estimated states are calculated as

$$\hat{X}_k = \hat{X}_{k|k-1} + K_k(y_k - C_k\hat{X}_{k|k-1}),\ \forall \hat{X}_{k|k-1} = \hat{X}(t_k) \quad (38)$$

4.2 Fault detection technique

In general fault diagnosis mechanism, a system fault is detected by evaluating fault information (set of sensor data, estimated unknown fault, etc.) through which 'fault detection' decision is made. Then the decision expression is conveyed as a Boolean indicator and defined as a *fault flag* $\in \{0,1\}$. For each *fault flag*, a recovery action has to be taken in order to avoid system instability. In this paper, the EKBUIO is implemented for sensor fault detection based on the estimation of fault information ' d_k^s '. Indeed, this estimated information d_k^s carries an unknown additive magnitude of the fault invoked in the sensor at each time step k. Consequently, memory and computational problems due to dealing with a vast amount of sensor/process data in probabilistic approach [38] or signal processing approach [39] can be avoided in the proposed fault detection technique.

It is obvious that, d_k^s should be zero when the sensor is out of the fault and the *fault flag* is set to zero. A decision of 'sensor fault' is made by triggering the *fault flag*=1 while $|d_k^s| > 0$. However in practice, modeling error, system uncertainty or un-modeled environment phenomenon are also considered as the unknown input in the sensor and may interfere with the estimation performance (the estimated error would be affected, (see (18)). These impacts are then reflected through the estimated d_k^s and directly affect the *fault flag* handling. Therefore in order to reduce this influence, a simple but effective solution is suggested by comparing d_k^s with a threshold value κ to set the *fault flag* as follows:

fault flag=1 if $|d_k^s| > \kappa$ (non-zero positive constant)
fault flag=0 otherwise

The value of the threshold κ is defined based on the system and environment characteristics. It needs to be selected carefully to cover only the modeling error and system uncertainties. If this threshold is too tight, a false alarm can be triggered not only by the original sensor fault, but also the modeling error or environmental influences (e.g. electro-magnetic interferences). On the other hand, if it is set to too large, original fault would be hidden. For both cases, the control performance can be degraded or suffers from instability. Hence, in our study, the reasonable value of κ has been selected based on trial-and-error method by investigating the system performance with its different settings. The selection procedure as well as the influence of different settings of κ on the system performance is clearly described in Section 5.1.3.

4.3 BELBIC controller design

In this paper, one of the recent innovated psycho-biological motivated brain emotional learning based intelligent controller (BELBIC) has been used for tracking control of EHA. Recent conducted researches [40, 41] revealed that how efficiently BELBIC can handle nonlinearities and uncertainties under noise and disturbances in EHA applications. The presented controller configuration is mainly based on a typical brain emotional model illustrated in Fig. 7.

In short, there are four main components in the BEL system. According to study [29], there are some Sensory inputs Si entering into Thalamus (Fig. 7(a)). In Thalamus, some simple pre-processes, such as noise reduction, are done [39]. Then the signals are sent to Amygdala and Sensory cortex. The Sensory inputs enter to Orbitofrontal cortex (OFC) as well. There is a digital memory type loop connection between Amygdala and OFC. Finally, the model output E is produced by Amygdala. Fig 7(b) represents the detailed configuration of these four blocks. In Amygdala, there exists a relationship between sensory inputs by a plastic and a learning path to each node 'A'. There is an additional node connected to Thalamus, is the maximum quantity of the Sensory inputs that is

$$S_{th} = \max(S_i) \quad (39)$$

Amygdala output A_i and OFC output O_i are calculated by (40) and (41), respectively.

$$A_i = S_i V_i \quad (40)$$

$$O_i = S_i W_i \quad (41)$$

DOI: XXX-XXX-XXXX

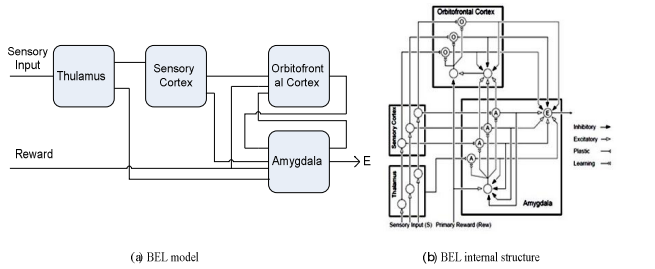

(a) BEL model (b) BEL internal structure

Fig. 7 General structure of a Brain Emotional Model (BEL)

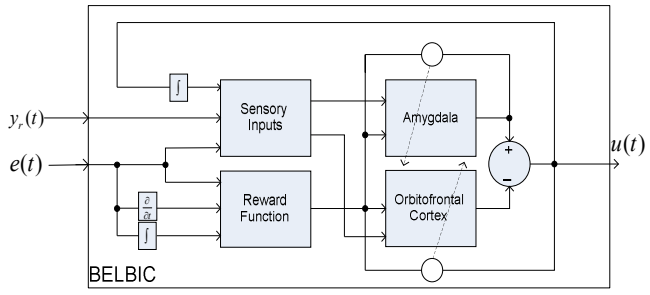

Fig. 8 BELBIC architecture for EHA position control

Here, the plastic weights of the Amygdala V_i and OFC W_i are evaluated by an associative learning system like Rescorla-Wagner model of learning:

$$\frac{\partial V_i}{\partial t} = \alpha.\left(\max\left(0, S_i.(Rew - \sum_i A_i)\right)\right) \tag{42}$$

$$\frac{\partial W_i}{\partial t} = \beta.\left(S_i.\max\left(0, \sum_j A_j - Rew\right) - \sum_i O_i\right) \; if \; Rew \neq 0$$
$$\frac{\partial W_i}{\partial t} = \beta.S_i.\max\left(0, \sum_j A_j - \sum_i O_i\right) \; if \; Rew = 0 \tag{43}$$

Here, A_j are all the Amygdala nodes except the Thalamus node; α and β are the learning rates of Amygdala and Orbitofrontal cortex individually; Rew is the 'Reward' function. Finally, the model output can be derived:

$$E = \sum_i A_i - \sum_i O_i \tag{44}$$

The 'max' functions in (42) ensures the Amygdala's monotonic learning. That is, once the emotional reaction is learned, it should be permanent. The OFC inhibits the inappropriate behavior of Amygdala. The OFC learning rule is similar to the Amygdala rule except that the plastic weights of this sector can increase and decrease.

In order to be used the BEL model as the controller – BELBIC, the reward function and Sensory inputs should contain some feedback signals, which are generally defined as

$$Rew = J(S_i, e, y_p)$$
$$S_i = f(u, e, y_p, y_r) \tag{45}$$

Illustration from (45), the reward function and Sensory inputs 'S_i' could be arbitrary functions of the reference input y_r, control input u, error e and plant output y_p. In common, a proper set of these functions and their weights are selected in order to increase the control performance [40].

5. Experiments

In this section, real-time experiments with tracking control of the EHA presented in Section 2 in faulty condition has been carried out to evaluate the designed FTC approach (Fig. 6) including the fault identification, fault detection and biologically inspired control (BELBIC). The control design procedure and verification process are then presented as bellows.

5.1 Experiment setting and control parameter design

5.1.1 BELBIC setting

To utilize the BELBIC for EHA tracking control, its structure is built as shown in Fig. 8. For designing the BELBIC as the main control module, the sensory inputs were carefully chosen as

$$S_i = \begin{pmatrix} 180e \\ 3\int u\,dt \\ 20y_r \end{pmatrix} \tag{46}$$

And the reward function can be selected as a formation of proportional-integral-derivative control form [40]. In this study, it was set as

$$Rew = 100e + 4\int e\,dt + 0.2\frac{de}{dt} \tag{47}$$

The learning rates were then selected as $\alpha = 0.0000003$ and $\beta = 0.000002$ for Amygdala and OFC respectively.

5.1.2 EKBUIO setting

The designed EKBUIO, expressed by from (33) to (38) in Section 3, observes the system pressure and position signals, P_l, P_h, P_r and y_k. The measurement matrix C and the fault distribution matrix E_m in (36) can be written as

$$C = \begin{bmatrix} 0 & 0 & 0 & 0 & 0 \\ 0 & 1 & 0 & 0 & 0 \\ 0 & 0 & 1 & 0 & 0 \\ 0 & 0 & 0 & 1 & 0 \\ 0 & 0 & 0 & 0 & 1 \end{bmatrix} \text{ and } E_m = \begin{bmatrix} 0 \\ 1 \\ 0 \\ 0 \\ 0 \end{bmatrix}$$

The process noise co-variance matrix, sensor noise co-variance matrix was considered as,

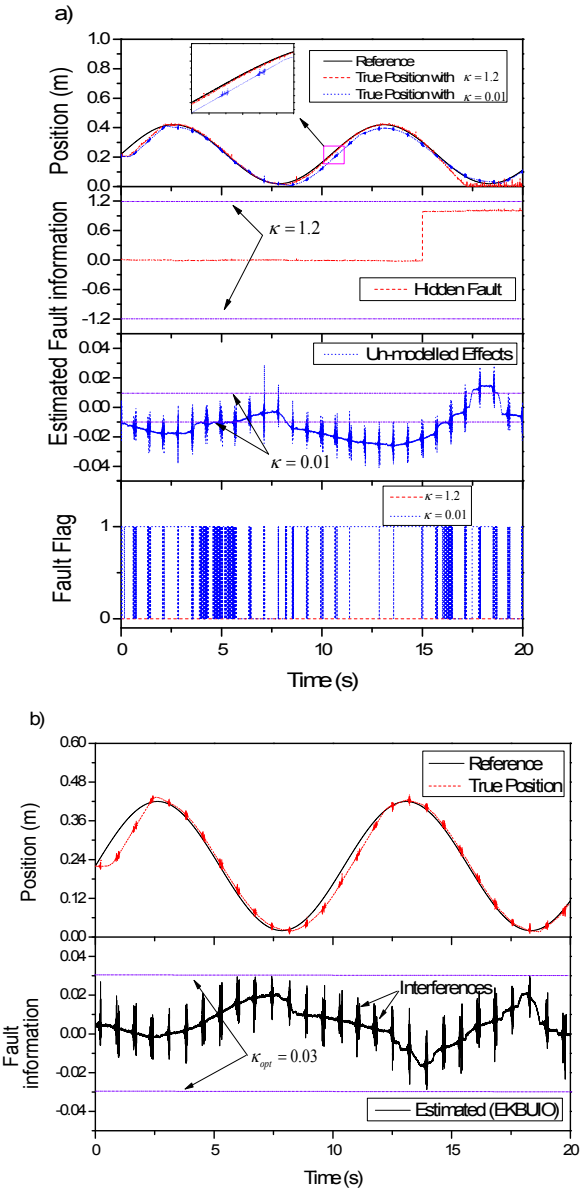

Fig. 9 System performance analysis: a) with different values of κ b) with optimal value of κ

$$Q_c^a = diag([10^{-10} \quad 10^{-12} \quad 10^{-10} \quad 10^{-10} \quad 10^{-10} \quad 2.25\times10^{-7}]$$
$$R_k = diag([.001^2 \quad .015^2 \quad 2^2 \quad 2^2 \quad 2^2])$$

5.1.3 Fault detection threshold setting

In order to distinguish between the original invoked fault and the un-modeled effects on the system, the fault detection threshold value κ was determined carefully by the experiment-based trial-and-error method. It is to be mentioned that, κ played an important role in this FTC performance. Fig. 9a shows an analysis of the effect of the threshold values on the system tracking results using the proposed FTC. With the large value, $\kappa = 1.2$, the FTC mechanism had low sensitivity. Thus, the system could track well the desired trajectory only when there was no fault existing.

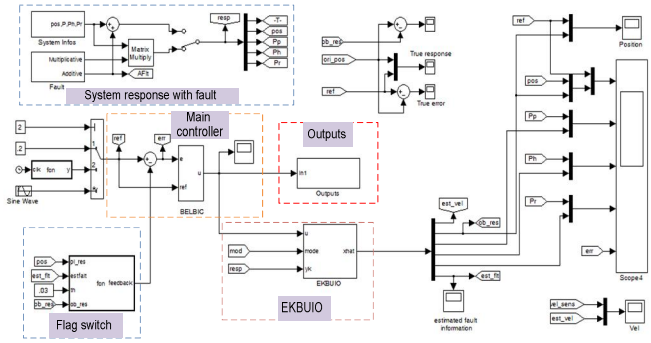

Fig. 10 Simulink control system using the proposed FTC

When the fault appeared, it was covered by the threshold value and the *fault flag* was not triggered. Subsequently, the system suffered from instability for this missed alarm (see the red-dash lines in the first, second and fourth sub-plots). On the other hand, with a small setting of $\kappa = 0.01$ the FTC mechanism was set to higher sensitivity. In this case, the system tracking performance was degraded. The reason was that the estimated fault information of the EKBUIO frequently passed the threshold value even there were only impacts of un-modelled terms. This, subsequently, resulted many wrong *fault flags* (see the blue-dot lines in the first, third and fourth sub-plots).

In order to find the optimum value of κ, firstly the *fault flag=0* was set, and then the system trajectory was controlled by the main controller under no-fault condition (See the first sub-plot of Fig. 9b). The estimated fault information can be observed as displayed in Fig. 9b (See the second sub-plot). As seen, it was bounded under 0.03 m, and $\kappa = 0.03$ was set in order to suppress this effect.

Finally, the designed control architecture was built in the Simulink environment combined with Real-time Windows Target toolbox of MATLAB as shown in Fig. 10. It has been then validated on the EHA systems in two faulty conditions: additive sensor fault case and multiplicative sensor fault case. Furthermore, a comparative study with a typical BELBIC closed-loop control (without FTC function) was also performed to clarify the ability of the proposed approach. The sampling period was set to 0.001 s for all experiments.

5.2 Experiment results

5.2.1 Control under additive sensor fault

For the first faulty case, the system was tested to track a sinusoidal trajectory with 0.7 Hz frequency and 0.4m amplitude under the additive sensor fault as depicted in Fig. 11. Here, additive fault was invoked into the controller feedback signal from time *t*=15 s as depicted in the third sub-plot of Fig. 11 with the solid-black line. The effect of this fault on the system performance is shown in the top sub-plot. As seen in this figure with the normal working condition, the BELBIC controller could drive the system adaptively.

DOI: XXX-XXX-XXXX

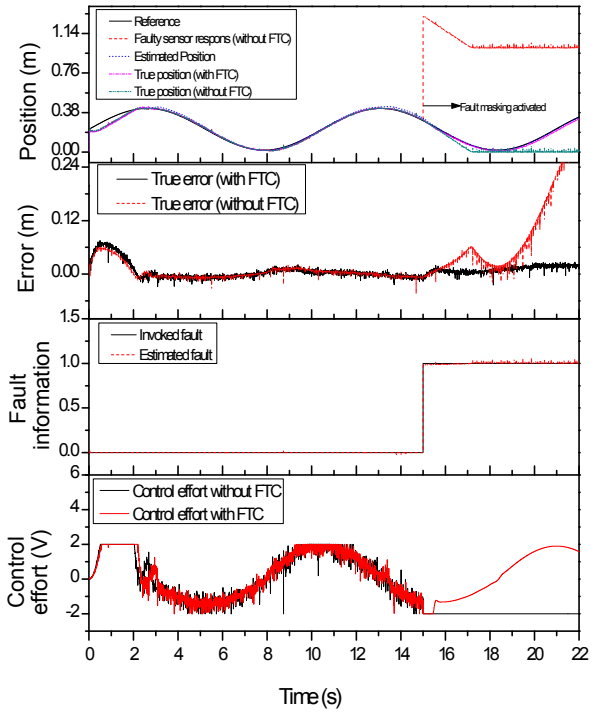

Fig. 11 Trajectory control with additive sensor fault

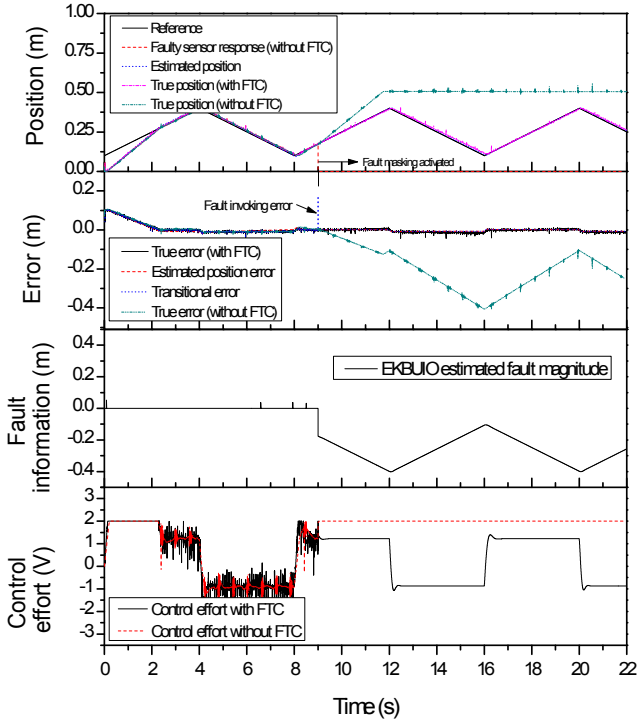

Fig. 12 Trajectory control with multiplicative sensor fault

However due to the lack of FDI ability, this controller could not retain the performance when existing any fault (as shown in the first and second sub-plots of Fig. 11 with the cyan-dash-dot-dot line and red-dash line, respectively). Without the FTC, the BELBIC got the wrong position information and subsequently, generated the wrong control effort which caused the system to be unstable with large tracking error. On the contrary by using the proposed control approach, the tracking performance was always kept in the acceptable range even existing any fault. It can be see that the control error in this case was only changed slightly when the fault happened (see the black-solid line in the second sub-plot). The reason is that the proposed method possesses not only the adaptability of the BELBIC module but also the sensor fault masking capability of the EKBUIO-based FDI module. The fault estimation result and control effort of this FTC method were in turn shown in the third and fourth sub-plots.

5.2.2 Control under multiplicative sensor fault

Next, the experiments with the second faulty case were then carried out. Here, a saw signal in the first sub-plot of Fig. 12 was used to represent the desired trajectory. The fault was generated by setting the position sensor gain to zero at t=9 s. Thus the sensor response to be zero suddenly and the position sensor can be considered as 100% failed (as shown in the first sub-plot of Fig. 12 with the red-dash-dot-dot line). Similarly to case 1, with the existence fault, the BELBIC without FTC architecture, could not be able to track the reference. Nevertheless, the designed FTC method still enhanced the acceptable tracking performance even facing fault (see black-solid line and the cyan-dash-dot-dot line of the third sub-plot respectively). Moreover, the estimated fault information of EKBUIO and good control effort of using this method are showed in the third and fourth sub-plots of Fig. 12 respectively.

Finally, the experiments were carried out with a multi-step tracking reference in the second faulty case. As the results obtained in Fig. 13, the fault was invoked by setting the sensor gain with 0.7 at t=12 s. That is the sensor was assumed to be degraded 30% of its current value (see the red-dash line of the first sub-plot of Fig. 13). With and without the FTC, the BELBIC tracks the trajectory in similar fashion. Meanwhile without the FTC system, the control error also degraded 30%. Because, the main control module could not have any fault information (see the red-dash line of second sub-plot). On the other hand, with FTC, the fault was detected quickly and continued the tracking operation with an acceptable accuracy (see the second sub-plot with black-solid line). The estimated fault information of the EKBUIO and the optimal control effort requirements are figured in the third and fourth sub-plots respectively (see the black-solid lines in each of the sub-plot).

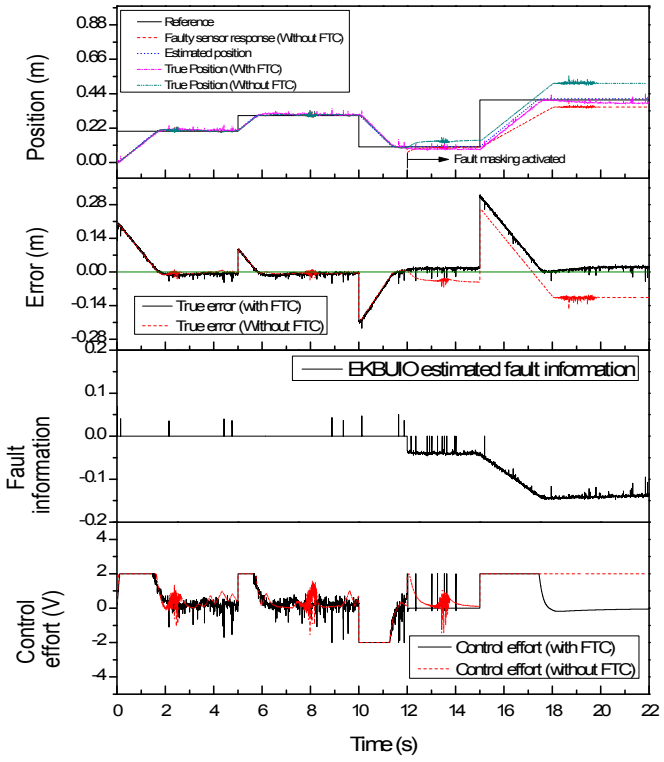

Fig. 13 Trajectory control under sensor performance degradation

6. Conclusions

In this paper, the fault tolerant control approach has been developed for tracking control of an electro-hydraulic actuator under sensor fault conditions. The proposed FTC is successfully designed as the combination of the main control module, BELBIC, and the fault detection and identification module. Here, the BELBIC is designed as a trajectory controller. Meanwhile, the EKBUIO-based FDI module estimates the system states and the unknown fault information.

In order to investigate the practical effectiveness of the developed FTC architecture, real-time experiments with position tracking control of the researched EHA using this logic have been carried out in case of existing additive and multiplicative sensor fault conditions. In addition, the comparative study with the BELBIC controller without FDI function was also performed to validate the advance of the proposed control method. The experimental results implied that the BELBIC controller could ensure the precise and stable performance when tracking the desired profiles in the normal working condition. However when facing with the faulty problems, only the suggested FTC architecture with the advanced design of the FDI module could retain the system stability. Meanwhile, the stability was totally degraded when using the conventional closed-loop system without this module. Our future research topics will be carried out on partial-model and non-model based robust fault tolerant control in different EHA driven industrial applications.

ACKNOWLEDGEMENT

This work was supported by the Technology Innovation Program (10043810, Development of a 20~40kW smart hybrid power pack for industry based on intelligent control) funded By the Ministry of Trade, Industry & Energy(MI, Korea) and by the Human Resource Training Program for Regional Innovation and Creativity through the Ministry of Education and National Research Foundation of Korea (NRF-2015H1C1A1035547).

REFERENCES

1. Kim, M.Y. and Lee, C.O. “An Experimental Study on The Optimization of Controller Gains For An Electro-Hydraulic Servo System Using Evolution Strategies,” J. of Control Engineering Practice, Vol. 14, pp. 137-147, 2006.
2. Rahmfeld, R. and Ivantysynova, M. “Displacement Controlled Linear Actuator With Differential Cylinder – A Way to Save Primary Energy in Mobile Machines,” In: Proceedings of The 5th International Conference on Fluid Power Transmission and Control, pp.316 –3,22 .2001
3. Zarei, J., and Shokri, E., “Robust Sensor Fault Detection Based on Nonlinear Unknown Input Observer,” Measurement, Vol. 48, pp. 355-367, 2014.
4. Pierri, F., Paviglianiti, G., Caccavale, F., and Mattei, M., “Observer-Based Sensor Fault Detection and Isolation for Chemical Batch Reactors,” Engineering Applications of Artificial Intelligence, Vol. 21, No. 8, pp. 1204-1216, 2008.
5. R., Petersen, I., and C., McFarlane, D., “A Methodology for Robust Fault Detection in Dynamic Systems,” J. of Control Engineering Practice, Vol. 12, pp. 123-138, 2004.
6. Hashemi, A., and Pisu, P., “Fault Diagnosis in Automotive Alternator System Utilizing Adaptive Threshold Method,” In: Proceedings of The Prognostics and Health Management Society, 2011.
7. F., Odgaard, P., and Stoustrup, J., “Unknown Input Observer Based Detection of Sensor Faults In A Wind Turbine,” In: Proceedings of The IEEE International Conference on Control Applications, pp. 310-315, 2010.
8. Zarei, J., and Poshtan, J., “Design of Nonlinear Unknown Input Observer for Process Fault Detection,” J. of Industrial & Engineering Chemistry Research, Vol. 49, No. 22, pp. 11443-11452, 2010.

DOI: XXX-XXX-XXXX

9. Giridhar, A., and El-Farra, N.H., "A Unified Framework For Detection, Isolation And Compensation of Actuator Faults in Uncertain Particulate Processes," Chemical Engineering Science, Vol. 64, No. 12, pp. 2963–2977, 2009.
10. Chengzhi, C., Weiguo, Z., and Xiaoxiong, L., "Application of Analytic Redundancy-Based Fault Diagnosis of Sensors to Onboard Maintenance System," Chinese Journal of Aeronautics, Vol. 25, pp. 236-242, 2012.
11. Isermann, R., "Model-Based Fault-Detection and Diagnosis – Status and Applications," Annual Reviews in Control, Vol. 29, pp. 71-85, 2005.
12. Puig, V., Quevedo, J., Escobet, T., Heras, S., "Passive Robust Fault Detection Approaches Using Interval Models," In: Proceedings of The 15th Triennial World Congress, Barcelona, Spain, 2002.
13. An, L., and Sepehri, N., "Hydraulic Actuator Circuit Fault Detection Using Extended Kalman Filter," In: Proceedings of The American Control Conference, Vol. 5, pp. 4261-4266, 2003.
14. Li, H., Yang, C., Hu, Y.G., Zhao, B., Zhao, M., and Chen, Z., "Fault-Tolerant Control for Current Sensors of Doubly Fed Induction Generators Based on an Improved Fault Detection Method," Measurement, Vol. 47, pp. 929-937, 2014.
15. Zarei, J., and Poshtan, J., "Sensor Fault Detection And Diagnosis of A Process Using Unknown Input Observer," J. of Mathematical and Computational Applications, Vol. 16, No. 1, pp. 31-42, 2011.
16. Alwi, H., Edwards, C. and Tan, C.P., "Fault Detection and Fault-Tolerant Control Using Sliding Modes," Springer, pp.7-27, 2011.
17. Chan, C. W., Jin, H., Cheung, K. C., and Zhang, H. Y., "Fault Detection of Systems With Redundant Sensors Using Constrained Kohonen Networks," Automatica, Vol.37, pp. 1671-1676, 2001.
18. Govindaraj, S. "Calculation of Sensor Redundancy Degree for Linear Sensor Systems," Master of Science thesis, University of Iowa, 2010.
19. Niksefat, N., and Sepehri, N., "A QFT Fault-Tolerant Control for Electrohydraulic Positioning Systems," IEEE Transactions on Control Systems Technology, Vol. 10, No. 4, pp. 626-632, 2002.
20. Mendonça, L.F., Sousa, J.M.C., and Da, Costa, S., "Fault Tolerant Control Using A Fuzzy Predictive Approach", J. of Expert Systems with Applications, Vol. 39, pp. 10630-10638, 2012.
21. Shang, W., Zhou, X., and Yuan, J., "An Intelligent Fault Diagnosis System for Newly Assembled Transmission" J. of Expert Systems with Applications, Vol. 41, pp. 4060-4072, 2014.
22. Fu, X., Liu, B., Zhang, Y., and Lian, L., "Fault Diagnosis of Hydraulic System in Large Forging Hydraulic Press," Measurement, Vol. 49, pp. 390-396, 2014.
23. Pisu, P., Rizzoni, G., and Serrani, A., "Model-Based Sensor Fault Detection and Isolation in A Steer-By-Wire System with Parameter Uncertainties," Technical Paper for Students and Young Engineers-Fisita World Automotive Congress, Barcelona, 2004.
24. Hossein, M., and Poshtan, J., "Fault Detection And Isolation Using Unknown Input Observers With Structured Residual Generation," Int. J. Instrumentation and Control Systems, Vol.2, No.2, pp. 1-12, 2012.
25. Sepasi, M., and Sassani, F., "On-line Fault Diagnosis of Hydraulic Systems Using Unscented Kalman Filter," Int. J. Control, Automation, and Systems, Vol. 8, No. 1, pp. 149-156, 2010.
26. Rezazadeh, A. S., Koofigar, H. R. and Hosseinnia, S., "Robust Leakage Detection for Electro Hydraulic Actuators Using an Adaptive Nonlinear Observer," Int. J. Precis. Eng. Manuf., Vol. 15, No. 3, pp. 391-397, 2014.
27. Sesha, K.D., and Gary, J.B., "Using Unknown Input Observers To Detect And Isolate Sensor Faults In A Turbofan Engine," In: Proceedings of The 19th Digital Avionics Systems Conference, Vol. 2, pp. 6E5/1-6E5/7, 2000.
28. Halder, P., "A Novel Approach for Detection and Diagnosis of Process and Sensor Faults in Electro-Hydraulic Actuator," Int. J. Engineering Research and Development, Vol. 6, No. 7, pp. 15-22, 2013.
29. Moren, J. and Balkenius, C., "A Computational Model of Emotional Learning in the Amygdala," J. of Cybernetics and Systems, Vol. 32, No. 6, pp. 611-636, 2000.
30. Shenouda, A., "Quasi-Static Hydraulic Control Systems and Energy Savings Potential Using Independent Metering Four-Valve Assembly Configuration," Ph.D thesis, Georgia Institute of Technology, 2006.
31. Jelali, M. and Kroll, A., "Hydraulic Servo-Systems Modelling, Identification and Control," Springer, pp.35-71, 2002.
32. Oh, J.Y., Jung, G.H., Lee, G.H., Park, Y.J. and Song, C.S. "Modeling And Characteristics Analysis of Single-Rod Hydraulic System Using Electro-Hydrostatic Actuator," Int. J. Precis. Eng. Manuf., Vol. 13, No. 8, pp. 1445-1451, 2012.
33. Mason, J.C. and Handscomb, D.C., "Chebyshev Polynomials," CRC Press, pp.145-150, 2002.
34. Chen, J., Patton, R. J., "Robust Model-Based Fault Diagnosis for Dynamic Systems," Kluwer Academic Publishers, pp. 19-33, 1999.
35. Chen, J., Patton and R. J., "Robust Fault Diagnosis of Stochastic Systems with Unknown Disturbances," In:

Proceedings of IEE International Conference on Control: Part 2, pp. 1340-1345, 1994.

36. Zarei, J., and Poshtan, J., “Design of Nonlinear Unknown Input Observer for Process Fault Detection,” Ind. Eng. Chem. Res., Vol. 49, No. 22, pp. 11443-11452, 2010.
37. Witczak, M., and Pretki, P., “Design of an Extended Unknown Input Observer with Stochastic Robustness Techniques and Evolutionary Algorithms,” International Journal of Control, Vol. 80, No. 5, pp. 749-762, 2007.
38. Robert, H. C., Hok, K. N., Jason, L. S., Lokeshkumar, S. G., and Russell, C., "Health Monitoring of a Satellite System", Journal of Guidance, Control, and Dynamics, Vol. 29, No. 3, pp. 593-605, 2006.
39. Hicham, T., Arezki, M., Abdelhalim, K., and Ridha, K., " Fast Fourier and discrete wavelet transforms applied to sensorless vector control induction motor for rotor bar faults diagnosis", ISA Transactions, Vol. 53, pp. 1639-1649, 2014.
40. Nahian, S. A., Truong D. Q., and Ahn K. K., "A Self-Tuning Brain Emotional Learning–Based Intelligent Controller for Trajectory Tracking of Electrohydraulic Actuator," Proceedings of the Institution of Mechanical Engineers, Part I: J. of Systems and Control Engineering, DOI: 10.1177/0959651814530275, 2014.
41. Sadeghieh, A., Sazgar, H., Goodarzi, K. and Lucas, C., “Identification And Real-Time Position Control of A Servo-Hydraulic Rotary Actuator By Means of A Neurobiologically Motivated Algorithm,” ISA Transactions, Vol. 51, pp. 208-219, 2012.